Chapter 12
Liquid Crystals and their Applications in the THz Frequency Range

Nico Vieweg, Christian Jansen and Martin Koch

Abstract We present a survey through the study of liquid crystals with terahertz time domain spectroscopy. The macroscopic dielectric properties such as the refractive index and the absorption coefficient for both ordinary and extraordinary polarization of various liquid crystals are presented and the underlying physical mechanisms are discussed. Furthermore, we deduce the microscopic characteristics such as the order parameter and the polarizabilities from the measured data.

Keywords Liquid Crystals · Birefringence · Order parameter · Molecular polarizabilities

12.1 Liquid Crystals at THz Frequencies

12.1.1 Introduction

Since Friedrich Reinitzer's discovery of the liquid crystals (LC) in 1888, a new age dawned in the understanding of the phases of matter [1]. Before this discovery, people had knowledge of only three phases, the solid, the liquid, and the gaseous state. At first, some scientists had many arguments against Reinitzer's proposal of the new phase. However, in the following years, other groups confirmed Reinitzer's findings. Thus, today the theory of this new state of matter is fully accepted.

The reason for the scientific interest in LCs lies in the unique combination of order, as known from a crystal and fluidity, as observed in a liquid. Moreover, many

M.Koch (✉) · N. Vieweg · C. Jansen
Department of Physics, Philipps-Universität Marburg, 35032Marburg, Germany
e-mail: martin.koch@physik.uni-marburg.de

C. Jansen
e-mail: chr.jansen@gmx.net

K.-E. Peiponen et al. (eds.), *Terahertz Spectroscopy and Imaging*,
Springer Series in Optical Sciences 171, DOI: 10.1007/978-3-642-29564-5_12,

LCs exhibit optical anisotropy and a strong response to magnetic or electric fields rendering them ideal candidates for tunable optical components. Today, liquid crystals have found their way into many optical applications, among which the liquid crystal display is certainly the most renowned. Recently, the large potential that LCs hold as base material for switchable terahertz (THz) devices has been discovered. However, to unchain this potential, a profound knowledge of their dielectric properties in the THz frequency regime is mandatory and an understanding of the physical mechanisms forming these properties has to be obtained.

12.1.2 State of the Art

Since the early 1970s, researchers have explored the far-infrared (FIR) properties of liquid crystals [2–18]. During these times and with the scientific instruments available, only limited information about the liquid crystal FIR properties were accessible. These methods include measuring the absorption coefficient with a Fourier Transform Infrared (FTIR) spectrometer or a CH_2F_2-based THz laser [18]. However, results on the THz refractive index at single frequencies have been presented only with the latter method [18].

Due to the major breakthrough of THz time domain spectroscopy (THz TDS) in the 1990s, a new interest in the subject of liquid crystals soon followed. With THz TDS, both the THz refractive index n and the absorption coefficient α can be precisely determined from the measured data over a broad frequency range. The first LC THz TDS measurements were made by Turchinovich et al. on PCH5 [19]. This report was followed by several papers published by Prof. Pan's group on 5CB, 6CB, 7CB, 8CB [20–25], PCH5 [20, 22], E7 [26, 27], and a ferroelectric liquid crystal [28]. THz data on 5CB have also been presented by Bonn et al. [29]. Using different spectroscopy techniques, Takanishi et al. and Nishizawa et al. studied P-8-PIMB and MBBA, respectively [30, 31]. Furthermore, our group has also contributed to the field with results on a liquid crystal polymer [32] as well as the macroscopic and microscopic THz properties of LCs such as 5CB, 6CB, 7CB, 8CB [33, 34], 5OCB, PCH5, PCH7 [34], BL037 [35], MLC7029, I52 and 1808 [36], which are also discussed later in this chapter. More recently, Trushkevych et al. reported on the THz properties of the nematic mixture LCMS-107 [37].

THz device concepts based on LCs have been proposed. Among them are magnetically and electrically switchable phase shifters [22, 26, 38–40], filters [22, 41, 42], polarizer [43], and gratings [44] as suggested by Prof. Pan's group. Zhang and coworkers reported recently on a tunable THz photonic crystal [45]. Our group furthermore demonstrated a LC-based dielectric THz-mirror and a sub-THz photonic crystal [46, 47]. Moreover, Khoo et al. suggested a tunable THz device, which combines a metamaterial with liquid crystals [48–50]. This concept has been put into practice by Werner et al. for the near infrared, by Bossard et al. for the THz frequency regime, and by Zhao et al. for the sub-THz range [48, 51–53]. More recently, Yuan et al. proposed an electrically controlled liquid crystal THz switch [54].

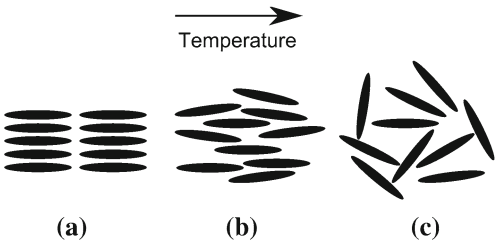

Fig. 12.1 **a** crystalline, **b** nematic and **c** isotropic phase of a liquid crystal

12.1.3 Liquid Crystals Phases

The most commonly employed liquid crystals, also known as calamitics, consist of rod-like molecules. This type can exhibit many different liquid crystal phases [55]. The simplest LC phase is called nematic (greek word for thread). In this phase, the molecules are randomly distributed but tend to align in a preferred direction. In other words, the material shows orientational, but no positional order. The phase transition of a nematic liquid crystal is illustrated in Fig. 12.1. A nematic liquid crystal changes its phase with increasing temperature from a well-ordered crystalline, to a less ordered nematic and finally, to a disordered isotropic liquid phase. From the application point of view, the nematic phase is favored because of the sensitive response of the molecules to electric fields.

12.1.4 Key Properties

Due to the long wavelength, THz devices require thicker LC layers compared to devices operating at optical frequencies, which implies slower switching times and higher losses [56]. For many LC devices the phase shifting capabilities is the major mechanism which is proportional to the product $\Delta n \cdot d$, where Δn is the THz birefringence and d the LC layer thickness. It is obvious that Δn needs to be large, if the layer thickness is supposed to be small. For this reason, the key properties for THz LCs are a high birefringence and a small absorption. Aside from switching times and losses, the stable operation temperature range can also be crucial depending on the application requirements.

12.1.5 Positive versus Negative Dielectric Anisotropy

The first LCs used in switchable optical devices were nematics with positive dielectric anisotropy (PDA). Those are also referred to as the classical LCs [56]. Because of their molecular structure comprising a polar head group, they exhibit a strong electric

dipole moment along the long axis. This property is important for the interactions of LCs with static or low frequency electric fields. PDAs always tend to align parallel to the electric field lines.

In negative dielectric anisotropic (NDA) LCs, the different dielectric anisotropic behavior is, for example, caused by the laterally substituted cyanide (CN) or fluorine (F) groups [57–59]. As a result, a strong permanent dipole moment is formed in the direction perpendicular to the molecular long axis. This dipole moment is of major importance for the interaction of NDAs with electric fields. While the classic PDA LCs prefer a parallel alignment, NDA LCs rather orient perpendicular to the static electric field.

12.1.6 Pure Liquid Crystals versus Mixtures

Depending on the application requirements, LCs need to have certain properties such as a high optical birefringence, a positive or negative dielectric anisotropy, low switching times, chemical stability, etc. However, those requirements are hard to fulfill by a pure substance. Therefore, the LC properties are optimized by mixing up to 20 different single LC components [56, 60–64]. Today, several different nematic mixtures have been developed. Among these mixtures are optimized ones for fast switching, low energy consumption, or high optical contrasts.

12.1.7 Macroscopic Properties – from kHz to UV

To develop a better understanding of the physical interactions of the liquid crystals with electromagnetic waves, we present the frequency-dependent dielectric parameters of 5CB, a member of the cyanobiphenyl (CB) family. The basic dispersion behavior of many nematic LCs is very similar [33], so that 5CB can serve as a representative example.

The frequency dependent refractive index afnd the absorption coefficient of 5CB are shown in Fig. 12.2a, b, respectively. In addition to the THz data obtained by the authors, data from the lower and higher frequency region, which were previously published by Gestblom et al., Weil et al., as well as Wu and Li are shown for comparison [65–68].

Considering the data presented in Fig. 12.2a, three different regimes can be identified. At kHz frequencies, the permanent dipole moment of the 5CB molecules still follows the electric field. Thus, a high birefringence and large values for the refractive index are observed. In the MHz frequency region the electric field becomes too fast for the permanent dipole to follow and a relaxation behavior sets in. During the relaxation the two curves for the ordinary and the extraordinary refractive index intersect twice. At these points the anisotropy completely vanishes. Starting at GHz frequencies and spanning up to the mid-infrared a steady decrease of both the

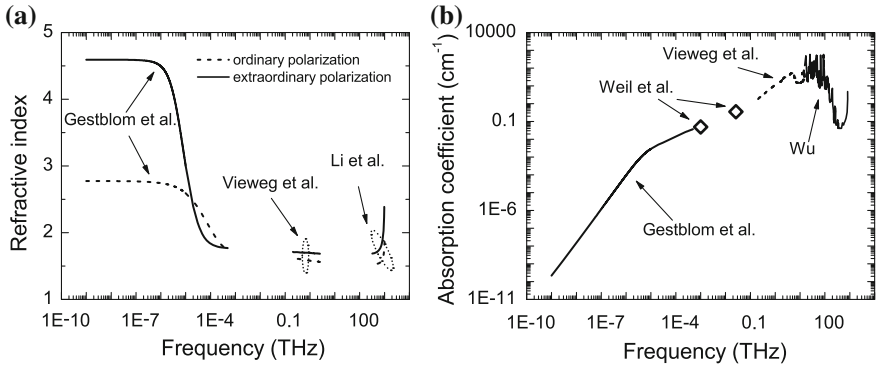

Fig. 12.2 Frequency-dependent refractive index **(a)** and mean absorption coefficient **(b)** of 5CB from microwaves to the visible (cf. [65–68])

ordinary and the extraordinary refractive index is found. The absorption spectrum presented in Fig. 12.2b shows an absorption band located at 5 THz [2] that is followed by strong vibrational absorption modes in the mid-infrared region, which lead to a strong resonance dispersion [67, 68]. The modes weaken in the NIR region (between 300 and 430 THz). In addition, the NIR region is not yet influenced by electronic transitions, which take place in the VIS and UV and strongly impact the dispersion characteristics in the high frequency regime.

12.1.8 THz Spectroscopy on Liquid Crystals

A standard THz time domain spectroscopy setup is employed to experimentally investigate the properties of the LCs over a broad frequency and temperature range [69–71]. Femtosecond pulses generated in a titan-sapphire laser, gate photoconductive antennas, which serve as THz emitter and detector [72]. The THz beam is guided by four off-axis parabolic mirrors with the sample positioned in the intermediate focus. The experiments are conducted in a nitrogen atmosphere to avoid water absorption lines in the spectra.

A liquid crystal cuvette consists of two THz transparent windows with 1.3 mm metal wire electrodes on two sides (Fig. 12.3). Materials such as fused silica, Topas, or high density polyethylene are appropriate window materials. While the plastics windows show a lower absorption, fused silica serves well if proper surface conditions or temperature control is required. To align the LCs, an electric 1 kHz AC field of $E_{\text{eff}} = 37\,\text{kV/m}$ is applied to the in-plane electrodes [73]. Measuring the extraordinary material parameters requires the molecular long axis to be aligned parallel to the polarization of the incident THz wave. In contrast, the ordinary parameters are obtained with the LCs long axis oriented perpendicular to the incident THz field

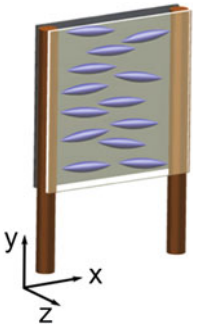

Fig. 12.3 Liquid crystal cuvette

Table 12.1 Liquid crystal material presented in this book chapter

	Pure LCs	Mixtures
PDAs	5CB, 5OCB, PCH5	BL037
NDAs	I52, 7CP7BOC	MLC7029, 1808

polarization. Peltier elements connected to a thermoelectric controller enable measurements of the material properties at different temperatures.

Extracting the material parameters from the measured data is a challenging task. The system under investigation has at least three layers. The material parameters change from layer to layer, resulting in reflections from the layer interfaces, which requires a more complex approach to the data analysis. To obtain highly precise material parameters from the measured data we use a novel data extraction algorithm. This algorithm accounts for the cuvette walls and multiple reflections of the THz pulse at the LC cell boundaries [74, 75]. The multilayer data extraction is also discussed in [76].

12.1.9 Macroscopic THz Properties of Liquid Crystals

In the following section, we present experimental results on the macroscopic properties of the LCs, e.g., the refractive index, the birefringence, and the absorption coefficient. Exemplary for the PDA class, we present data on the cyanobiphenyl 5CB, the phenyl-cyclohexane PCH5, the pentyloxy-cyanobiphenyl 5OCB, and the nematic mixture BL037. As representatives for the NDAs, we investigate four substances among which I52 and 7CP7BOC are pure substances, while MLC7029 and 1808 are two nematic mixtures. The LC materials presented within the scope of this chapter are summarized in Table 12.1.

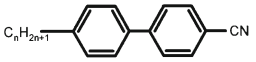

Fig. 12.4 Chemical structure of the cyanobiphenyls. The molecules consist of an alkyl chain (C_nH_{2n+1}), a cyanide head (CN), and a biphenyl core. The index n indicates the number of C atoms in the side chain. The polar cyanide head causes a dipole moment along the molecular long axis

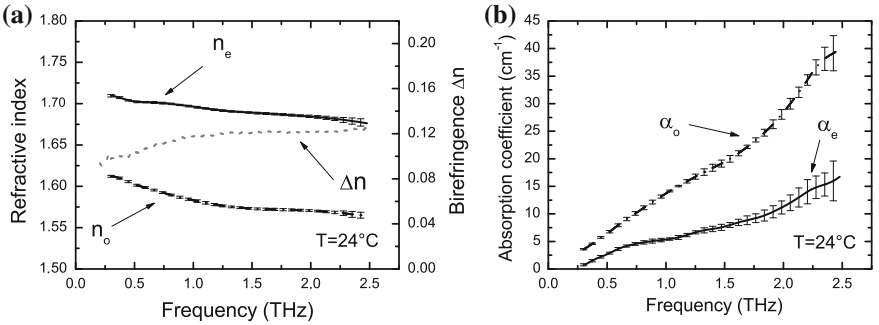

Fig. 12.5 **a** Refractive index and birefringence and **b** absorption coefficient for both ordinary and extraordinary polarization of 5CB at 24 °C

12.1.9.1 Cyanobiphenyl 5CB

Room temperature operation is an important requirement of the LCs used for devices. Cyanobiphenyls, first developed by Gray and coworkers in 1973 [77], offer this property. CBs are ideal candidates for spectroscopic studies, as they are widely available and well characterized.

The chemical structure is depicted in Fig. 12.4. CBs consist of a biphenyl core with a cyanide head (CN) on one and an alkyl chain (C_nH_{2n+1}) on the other side. The index n indicates the number of C atoms in the side chain.

As a representative member of this group we chose 5CB for further investigation. The THz refractive indices n_o and n_e and absorption coefficients α_o and α_e at 24 °C for ordinary and extraordinary polarization are depicted in Fig. 12.5. In comparison, the extraordinary is always larger than the ordinary refractive index ($n_e > n_o$), whereas the absorption coefficient is always larger for ordinary polarization ($\alpha_o > \alpha_e$). For example, the values of the refractive indices at 2 THz are $n_e = 1.69$ and $n_o = 1.57$ and the corresponding absorption coefficients are $\alpha_e = 13\,\mathrm{cm}^{-1}$ and $\alpha_o = 28\,\mathrm{cm}^{-1}$. The birefringence of 5CB at 2 THz is 0.12. The parameter for extraordinary refraction decreases slightly with the frequency, while there is a larger gradient for the ordinary axis. Both the ordinary and extraordinary absorption coefficients rise with the frequency, but there is a stronger increase for the ordinary axis.

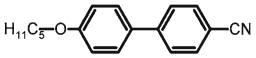

Fig. 12.6 Chemical structure of 5OCB. The molecule contains an alkoxy group ($C_nH_{2n+1}O$), a cyanide head (CN), and biphenyl core

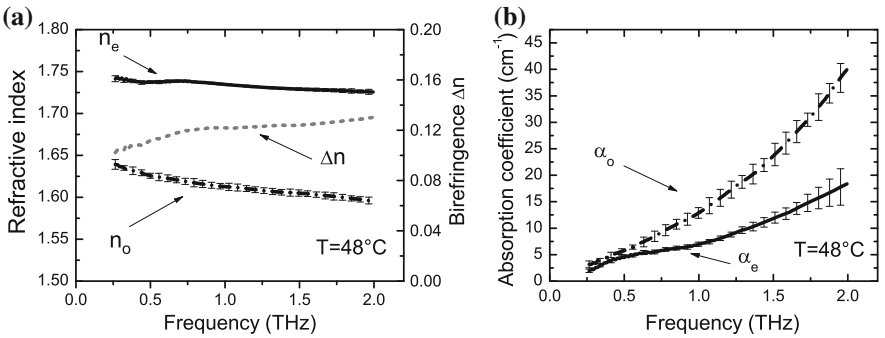

Fig. 12.7 **a** Refractive index and birefringence and **b** absorption coefficient both for ordinary and extraordinary polarization of 5OCB at 48 °C

12.1.9.2 Pentyloxy-Cyanobiphenyl 5OCB

Pentyloxy-cyanobiphenyls (OCBs) share the same basic structure with their CB relatives comprising a biphenyl core, a cyanide head, and an alkyl chain. In contrast to CBs, the alkyl chain in case of the OCBs is linked via an oxygen atom to the core (also called alkoxy chain). The additional oxygen makes the molecule less flexible, which results in a drastic shift of the nematic phase toward higher temperatures. Although 5OCB reaches the nematic phase starting at 48 °C, it exhibits a stability of the nematic phase over a broad temperature range.

The THz material parameters of 5OCB are shown in Fig. 12.7. The additional oxygen atom has only a weak effect on the THz anisotropy. The birefringence is with $\Delta n = 0.13$ at 2 THz only slightly higher than the birefringence of 5CB. The absorption behavior is also quite similar. Compared to 5CB a marginally higher absorption is found.

12.1.9.3 Phenylcyclohexane PCH5

Briefly after the discovery of the CBs, Eidenschink et al. introduced a new liquid crystal family called phenylcyclohexanes (PCHs) [78–80]. In general, PCHs differ from CBs in their core structure, which is shown in Fig. 12.8. While CBs consist of two phenyl rings, the PCHs contain a cyclohexane instead of one of the phenyl rings. PCHs are favored for some applications, as they exhibit a better chemical stability and a broader nematic range than the CBs. They are often employed as a reference material, e.g. for calibration purposes [78–80].

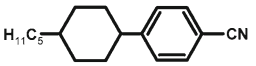

Fig. 12.8 Chemical structure of the phenyl-cyclohexanes. The molecule consist of an alkylchain (C_nH_{2n+1}), a cyanide head (CN), and a combination of phenyl and cyclohexane ring in the core

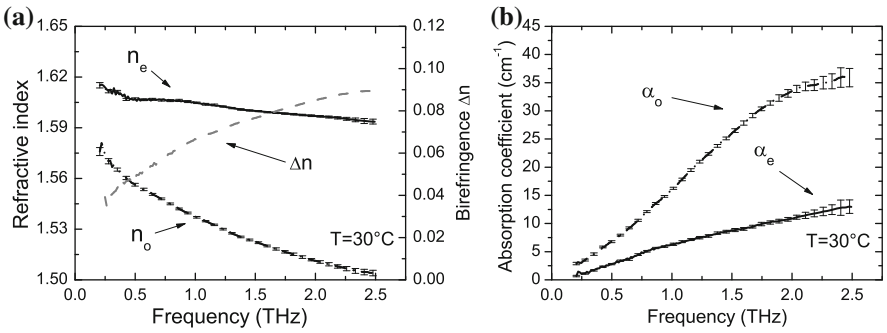

Fig. 12.9 **a** Refractive index and birefringence and **b** absorption coefficient both for ordinary and extraordinary polarization of PCH5 at 30 °C

From their optical properties it is known that PCHs exhibit only a small anisotropy because of the short conjugation length. In the THz range, a similar relation can be observed. The THz birefringence of PCH5 with $\Delta n = 0.08$ at 2 THz is smaller than the birefringence of 5CB. The material parameters of PCH5 are presented in Fig. 12.9. The refractive indices are for instance $n_e = 1.59$ and $n_o = 1.51$ at 2 THz and 30 °C. In general, the PCHs show a similar dependence on the frequency as the CBs and OCBs.

The presented pure LCs all show a very similar behavior. They exhibit a rather small birefringence and a large absorption at higher THz frequencies. In general, this makes them less attractive for use in THz devices. While the extraordinary absorption coefficient increases only to some extent, we find a strong rise for the ordinary excitation. The absorption in this region is caused by strong torsional motions which lead to a broad absorption band located around 5 THz [2–18]. The absorption band is always larger for the ordinary than for the extraordinary excitation. We attribute this phenomenon to the fact that the rod-like liquid crystals can move easier around their long axis than around the two short axes. Thus, molecular vibrations excited by extraordinary waves are more hindered, which results in a weaker absorption.

12.1.9.4 Nematic Mixture BL037

In order to find a more suitable candidate for THz applications, this section examines the properties of BL037, a mixture that has been optimized with regard to the optical anisotropy. For the optical frequency region the properties are specified to be

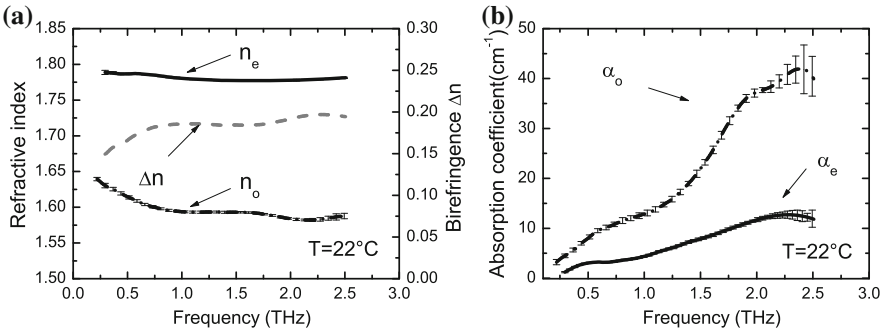

Fig. 12.10 **a** Refractive indices and **b** Absorption coefficients of BL037 at 22°C for ordinary and extraordinary polarization

$\Delta n|_{589\,\mathrm{nm}} = 0.282$, $n_e|_{589\,\mathrm{nm}} = 1.808$, $n_o|_{589\,\mathrm{nm}} = 1.526$. Here, Δn specifies the optical anisotropy and n_e and n_o represent the optical refractive indices. The mixture consists of the known cyanobiphenyls (CBs and OCBs), which are substituted with alkyl or alkoxy groups. In addition, BL037 contains substances with three rings in the core. The core either consists of three directly linked phenyl rings (terphenyl) or it is a combination of a biphenyl and a cyclohexane ring. We will further refer to both substances as TPs and BCs, respectively. TPs are liquid crystals that have a high optical anisotropy due to the good polarizability of this ring system (W. Becker, Merck KGaA). The mixture of these substances combines a high birefringence with a stable nematic phase of about −40 °C up to 109°C.

The THz material parameters are shown in Fig. 12.10. The birefringence rises with the frequency from $\Delta n = 0.18$ at 0.5 THz to $\Delta n = 0.2$ at 2 THz and is therefore twice as large as the birefringence of the CBs. While the extraordinary refractive index $n_e = 1.78$ remains relatively constant, the ordinary refractive index decreases slightly from $n_o = 1.6$ at 0.5 THz to $n_o = 1.58$ at 2 THz. The absorption coefficient for the ordinary and the extraordinary polarization are presented in Fig. 12.10b. Within the examined range both coefficients increase with the frequency and as before the ordinary absorption is higher and more dispersive than the extraordinary absorption.

In conclusion, we find that the mixture combines a broad temperature operation range and a high terahertz birefringence. Thus, BL037 is a good candidate for switchable THz devices. However, the absorption coefficient for ordinary excitation rises drastically with the frequency and limits the use of BL037 to the frequency range below 1 THz.

12.1.9.5 I52

As a member of the negative dielectric anisotropy LCs, we investigate 4-ethyl-2-fluoro-4′-[2-(trans-4-n-pentylcyclohexyl)-ethyl]-biphenyl (I52) [80, 81]. The molecule is composed of two phenyl and one cyclohexane ring (Fig. 12.11). While the

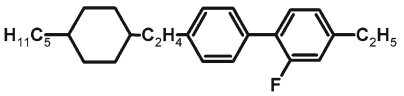

Fig. 12.11 Chemical structure of I52. A flourine atom is linked laterally to the outer phenyl ring, thus forming a dipole moment perpendicular to the molecular long axis

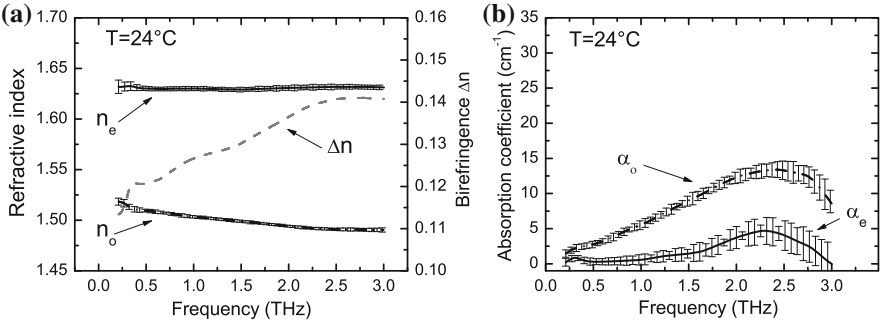

Fig. 12.12 **a** Refractive indices and **b** absorption coefficients for I52 at 24 °C for ordinary and extraordinary polarization. The permanent dipole moment is created by a laterally connected fluorine atom

two phenyl rings are linked directly, the cyclohexane ring and the biphenyl system are connected via a C_2H_4 group. At both ends I52 is terminated by two alkyl chains (C_5H_{11}, C_2H_5). The negative dielectric anisotropy is formed by a fluorine atom, which is linked in a lateral position to the outer phenyl ring.

Due to the high stability of the material parameters over a broad temperature range from 24 to 103.4 °C, I52 is often employed for instrumental calibration purposes [80]. The most important properties of I52 at a temperature of $T = 20\,°\text{C}$ are $\Delta n|_{589\,\text{nm}} = 0.1459$, $n_e|_{589\,\text{nm}} = 1.6495$ and $n_o|_{589\,\text{nm}} = 1.5036$, where Δn is the birefringence and n_o and n_e the refractive indices for ordinary and extraordinary polarization.

Figure 12.12 shows the extracted THz material parameters. The extraordinary refractive index remains constant, while the ordinary parameter decreases with increasing frequency. As an example, the refractive indices at 2 THz are 1.49 and 1.63 for ordinary and extraordinary polarization, respectively. Both indices differ only slightly from the values reported for the optical frequency range. The average value of the THz birefringence is $\Delta n = 0.14$ and thus only slightly smaller than the optical value of 0.1459. Thus, I52 shows a larger birefringence than its PDA relatives, e.g., the cyanobiphenyls.

12.1.9.6 7CP7BOC

The second NDA LC is called 2-chloro-4-n′-alkylphenyl esters of 4-n-alkylbicyclo [2,2,2] octane-1-carboxylic acid, to which we will further refer to as 7CP7BOC (Fig. 12.13). It consists of a phenyl ring and a bicyclooctane ring. Both rings are linked

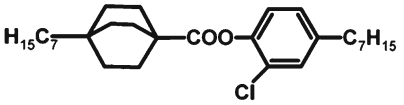

Fig. 12.13 Chemical structure of 7CP7BOC. A cyanide group is connected at a lateral position, resulting in a dipole moment perpendicular to the molecular long axis

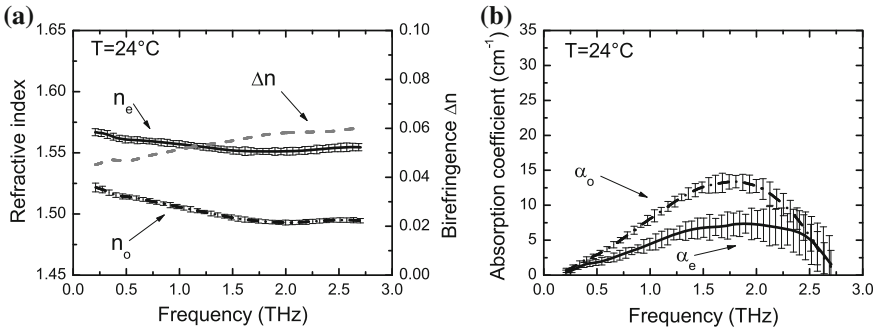

Fig. 12.14 **a** Refractive indices and **b** absorption coefficients for 7CP7BOC at 24 °C for ordinary and extraordinary polarization. The permanent dipole moment is created by a laterally linked cyanide (CN) group

by an ester group (COO) and terminated with a heptyl chain. In contrast to I52, the permanent dipole moment is formed by a chlorine atom linked laterally to the phenyl ring. The optical properties of 7CP7BOC are reported to be $\Delta n|_{589\,\mathrm{nm}} = 0.064$, $n_e|_{589\,\mathrm{nm}} = 1.5574$ and $n_o|_{589\,\mathrm{nm}} = 1.4932$ [82, 83].

The THz material parameters are presented in Fig. 12.14. On average, the THz birefringence of 7CP7BOC $\Delta n = 0.06$ is less than half the value of the birefringence of I52, which is caused by the shorter conjugation length. The refractive indices for both polarization decrease at first slightly but remain nearly constant above 2 THz. As an example, the refractive indices at 2 THz are measured to be 1.49 and 1.55 for ordinary and extraordinary polarization, respectively. From this result we see that the THz-values for the refractive indices are very close to the optical values.

As for I52, a broad absorption band is observed at frequencies around 2 and 2.3 THz for both polarizations of the THz wave. In the investigated frequency range, the ordinary absorption coefficient is always larger than the extraordinary parameter. In this regard, NDAs can be put on a level with PDAs.

Similar to I52, 7CP7BOC is also much more transparent than the above-mentioned classic PDA LCs. Obviously, the dipole direction has a strong impact on the THz properties. A molecule with a lateral permanent dipole seems to favor more damped oscillations around the long axis, which reflects in a lower absorption coefficient.

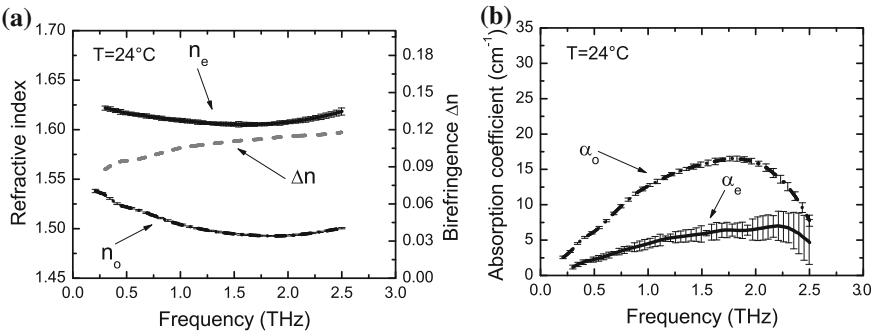

Fig. 12.15 **a** Refractive indices and **b** absorption coefficient of MLC7029 at 24 °C for ordinary and extraordinary polarization

12.1.9.7 Nematic Mixture MLC7029

In order to find further evidence of the dipoles impact, we investigated two nematic mixtures with negative dielectric anisotropy.

We first present THz measurements on MLC7029, which is a mixture optimized for fast switching cycles [56, 84]. The optical properties at 20 °C of MLC7029 are specified to be $\Delta n|_{593\,\mathrm{nm}} = 0.1265$, $n_e|_{593\,\mathrm{nm}} = 1.6157$ and $n_o|_{593\,\mathrm{nm}} = 1.4892$. In accordance to the optical properties, MLC7029 shows a moderate average birefringence of $\Delta n = 0.11$ at THz frequencies. The refractive indices decrease first with the frequency but increase again above 2 THz. As an example, the indices are determined to be 1.49 and 1.61 at 2 THz for ordinary and extraordinary polarization, respectively. At frequencies around 1.8 THz, MLC7029 shows a broad absorption band, similar to the one of the above presented NDA LCs.

12.1.9.8 Nematic Mixture 1808

The second mixture investigated is 1808. Like its PDA counterpart (BL037), 1808 is designed to have a high optical birefringence. The mixture consists of difluoroalkylterphenyls and alkyl-alkoxytolanes [59, 62, 85] (Roman Dabrowski, Military Technical Academy of Warsaw). Its THz properties are presented in Fig. 12.15. The absorption spectrum of 1808 appears to be more complex. However, the exact recipe is not publically available from the manufacturer and thus it is not possible to finally explain the absorption features here.

The mixture 1808 shows a high birefringence of $\Delta n = 0.2$ at 2 THz. The refractive indices are 1.52 and 1.72 at 2 THz for ordinary and extraordinary refraction, respectively. In comparison, the PDA mixture BL037 has some advantage over 1808 at lower frequencies (0.5–1.2 THz). At higher frequencies a similar birefringence is observed. However, 1808 exhibits a significantly smaller THz absorption.

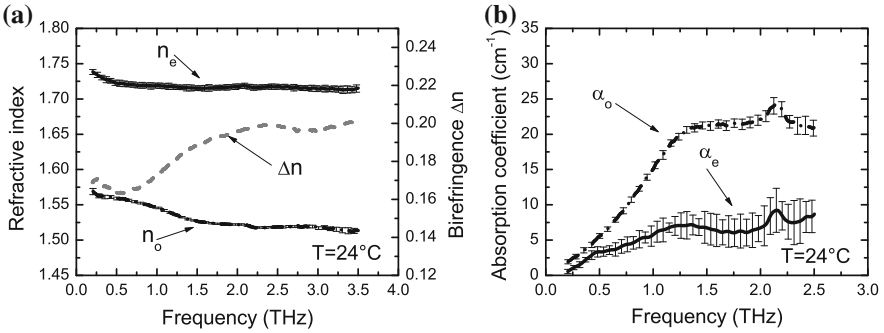

Fig. 12.16 **a** Refractive indices and **b** absorption coefficient of 1808 at 24 °C for ordinary and extraordinary polarization

Table 12.2 Birefringence and refractive indices at 2 THz for ordinary and extraordinary polarization of the Liquid Crystal material presented in this chapter

	n_o	n_e	Δn
5CB	1.57	1.69	0.12
5OCB	1.6	1.73	0.13
PCH5	1.51	1.59	0.08
BL037	1.58	1.78	0.2
I52	1.49	1.63	0.14
7CP7BOC	1.49	1.55	0.06
MLC7029	1.49	1.61	0.12
1808	1.52	1.72	0.2

Regarding their birefringence, the pure NDA substances as well as the mixture MLC7029 exhibit a behavior similar to their PDA counterparts. Yet, NDA LCs outperform the PDA LCs with regard to transparency, which we attribute to the different direction of the permanent dipole. The mixture 1808 surpasses the anisotropy of the other LCs by nearly a factor of two. Moreover, 1808 exhibits a lower overall absorption than the PDA mixture BL037 rendering 1808 an excellent choice for THz devices.

To summarize the macroscopic properties of the LCs presented above, the birefringence and the refractive indices for ordinary and extraordinary polarization at 2 THz are given in Table 12.2.

12.1.10 Molecular THz Properties of Cyanobiphenyls

After having considered the macroscopic properties of LCs, this section is dedicated to the investigation of the molecular characteristics of the cyanobiphenyls (CBs) at THz frequencies [73].

Table 12.3 Temperatures for the crystal/nematic (T_{CN}) and the nematic/isotropic phase transition (T_{NI}) as well as the reduced temperature $T_{CN} - T_{NI}$. Ref. [86]

	T_{CN} (°C)	T_{NI} (°C)	$T_{NI} - T_{CN}$ (K)
5CB	24	35.3	11.3
6CB	14.4	30.2	15.8
7CB	30.1	42.9	12.8

First, we will examine the cyanobiphenyls' molecular structure and its implications on the dielectric characteristics of 5CB, 6CB, and 7CB. Finally, an investigation of the anisotropy of the refractive index, the order parameter *S* as well as the principle and the main polarizabilities will be undertaken along with an interpretation of the underlying physical mechanisms.

12.1.10.1 The Molecular Structure of 5CB, 6CB, and 7CB

In contrast to many other commercially available LCs, the molecular structure of CBs is well known so that experimental observations can directly be linked to features of the molecular structure. The cyanobiphenyls consist of an alkyl chain ($H_{2n+1}C_n$) with a polar cyanide head group (*CN*), and a rigid core unit formed by a conjugated phenyl ring system. The molecules under investigation consist of the same basic structure and only differ in the length of the alkyl side chain (Fig. 12.4, 12.17).

At increasing temperatures the CBs undergo phase changes from a well-ordered crystalline to a less ordered nematic and finally to a disordered, isotropic phase (Table 12.3). A summary of the corresponding phase transition temperatures T_{CN} and T_{NI} as well as the reduced temperature T_{CN}-T_{NI} can be found in Table 12.3.

Among the cyanobiphenyls under investigation, two fundamental dependencies can be found: First of all, the differing alkyl chain lengths result in alterations regarding certain physical properties such as the polarizability and the density, which reflect in the anisotropy of both the absorption and the refractive index. Furthermore, aside from the total chain length, odd and even numbers of C atoms in the alkyl chain lead to a different macroscopic behavior [87–94].

From a thermodynamic point of view, the LC system tries to reach the lowest energy conformation in order to establish an equilibrium. For an odd number of C atoms, e.g., in 5CB or 7CB, this state of lowest energy is present when the tail is rather aligned in a *trans*-conformation along the principle long axis *m* (Fig. 12.17). In contrast, CBs with an even number of C atoms, e.g., 6CB reach the lowest energy state when the angle between the last C atom and the axis m becomes large (e.g. $\beta_{6CB} = 66.1°$) [88].

The different conformation behavior of odd- and even numbered CBs is also reflected in differing molecular properties, which is known as the odd and even effect [87–94]. In the following sections, the odd and even effect at THz frequencies

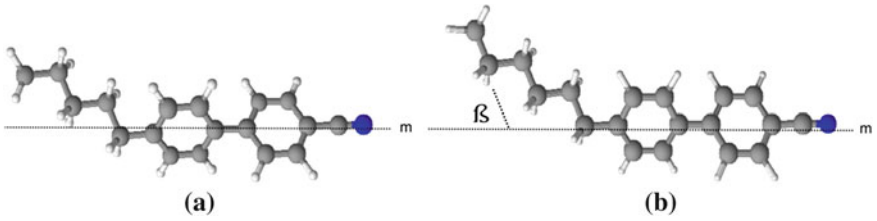

Fig. 12.17 Molecular structure of **(a)** 5CB and **(b)** 6CB. A large angle is formed between the last member of the alkyl chain and the long axis for the LCs with an even number of C atoms in the chain (6CB)

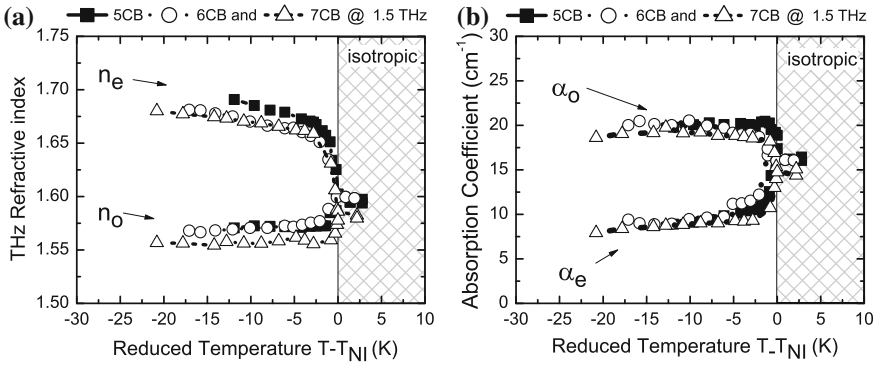

Fig. 12.18 **a** Refractive index and **b** absorption coefficient at 1.5 THz versus the reduced temperature for 5CB, 6CB, and 7CB

will be further investigated by studying the anisotropy of the refractive index *n,* the absorption coefficient α, and the order parameter *S*.

The frequency dependence of the refractive index and the absorption coefficient of 5CB have been presented further above. For the extraction of microscopic properties the temperature dependence is also required. Thus, we move on to investigating the temperature dependence of these parameters for 5CB, 6CB, and 7CB at a fixed frequency of 1.5 THz. Fig. 12.18 shows the refractive index and the absorption coefficient of the three materials. For a clear comparison of the three LCs, the x-axis is given in form of the reduced temperature $T\text{-}T_{NI}$, where T_{NI} is the temperature at which the transition between the nematic and the isotropic phase occurs (cf. Table 12.3). As expected, the strong polarizability of the LCs in direction of the long molecular axis results in a positive anisotropy (i.e. $n_e > n_o$) of the THz refractive index over the entire nematic phase. The transition between the nematic and the isotropic phase is clearly visible. However, the CBs do not exhibit a change in the material parameters at the transition between the nematic and the crystalline phase.

As the nomenclature suggests, the number of C atoms in the alkyl chain increases from five in case of 5CB to seven in case of 7CB. The density exhibits the inverse behavior with 5CB being the densest material with the highest number of molecules

per unit volume. Thus, 5CB also exhibits the highest refractive index, both in the ordinary and the extraordinary axis, of all the CBs investigated here.

Both 5CB and 7CB possess an odd number of CH_2 groups. Hence, a complete alignment of the tail along the molecular long axis according to the odd and even rule mentioned before can be observed. The two additional CH_2 groups in case of 7CB contribute to the polarizability of the long axis, which leads to an enhanced birefringence. Here, $\Delta n_{5CB} = 0.11$ and $\Delta n_{7CB} = 0.12$ at $T\text{-}T_{NI} = -10\,\mathrm{K}$.

Although the substance 6CB has the second longest tail and is thus the second densest material, its refractive index does not fit with respect to the refractive indices of 5CB and 7CB. Here, the last CH_2 group forms a large angle to the molecular long axis. Therefore, the birefringence is reduced to a value of $\Delta n_{6CB} = 0.10$ as the additional CH_2 group primarily contributes to the polarizability of the molecular axis perpendicular to the long axis. As the birefringence only slightly differs between the CBs, the reader is referred to the following section, where the anisotropy is again discussed with regard to the polarizabilities.

The absorption coefficient shown in Fig. 12.18b exhibits a pronounced linear dichroism. THz waves oriented along the ordinary direction excite a broad torsional vibration mode located around 5 THz [2–18]. Thus, the absorption α_o observed in the ordinary axis is higher than the absorption α_e observed in the extraordinary axis.

12.1.10.2 The Relation between Macroscopic and Molecular Data

Molecular properties, such as the longitudinal and the transverse contributions of the polarizability tensor, are of fundamental interest. However, above absolute zero, the intrinsic thermal energy is the source of a certain degree of disorder in the LC, resulting in the inability of spectroscopic measurements to directly give access to these molecular characteristics. Still, with the order parameter S known, a relation between the spectroscopic data and these molecular properties can be derived as follows [95, 96]:

$$(\zeta_e - \zeta_o) = S(\gamma_\parallel - \gamma_\perp) \tag{12.1}$$

In this equation, ζ_e and ζ_o stand for the principle polarizabilities, S for the order parameter, and $\gamma_\parallel$ and $\gamma_\perp$ for the longitudinal and transverse polarizability components of the perfectly ordered LC. The main polarizabilities $\gamma_\parallel$ and $\gamma_\perp$ can then be extracted using the equations:

$$\gamma_\parallel = \overline{\zeta} + \frac{2}{3S}(\zeta_e - \zeta_o) \tag{12.2}$$

and

$$\gamma_\perp = \overline{\zeta} - \frac{1}{3S}(\zeta_e - \zeta_o) \tag{12.3}$$

Here, the mean polarizability is given by

$$\bar{\zeta} = \frac{1}{3}\zeta_e + \frac{2}{3}\zeta_o \tag{12.4}$$

To proceed with our study of the molecular properties of the CBs we will perform the following steps: First, we extract the principle polarizabilities ζ_e and ζ_o by applying Vuks' approximation to the refractometric data [97, 98]. Then, we will determine the order parameter S by using Haller's extension to Vuks' approach. Finally, on the basis of this data we will be able to determine the main polarizabilities $\gamma_\parallel$ and $\gamma_\perp$.

12.1.10.3 Principle Polarizability

The first step of Vuks approach to deriving the polarizability of anisotropic materials from their refractive index is a generalization of the Lorentz–Lorenz formula [99, 100],

$$\frac{n_{e/o}^2 - 1}{n_{e/o}^2 + 2} = \frac{4\pi}{3} N \zeta_{e/o} \tag{12.5}$$

Here, n denotes the refractive index, N is the number of molecules per unit volume, and $\zeta_{e/o}$ represents the polarizability along the extraordinary and the ordinary polarization, respectively [101]. Vuks assumed that the mean refractive indices of anisotropic molecules in the crystalline state can be treated as isotropic media so that equation (12.5) remains valid. On this basis he derived

$$\frac{n_{e/o}^2 - 1}{\bar{n}^2 + 2} = \frac{4\pi}{3} N \zeta_{e/o}, \tag{12.6}$$

where $\bar{n}^2 = \frac{1}{3}n_e^2 + \frac{2}{3}n_o^2$ is the mean square of the refractive index. In Fig. 12.19a, the principle polarizability of 5CB, 6CB, and 7CB at 1.5 THz as predicted by Vuks' calculations is shown.

The LCs exhibit an anisotropy of the polarizability of $\Delta\zeta_{5CB} = 7.7 \times 10^{-24}\,\mathrm{cm}^3$, $\Delta\zeta_{6CB} = 7.2 \times 10^{-24}\,\mathrm{cm}^3$, and $\Delta\zeta_{7CB} = 8.8 \times 10^{-24}\,\mathrm{cm}^3$ at $T\text{-}T_{NI} = -10\,\mathrm{K}$ for 5CB, 6CB, and 7CB, respectively. As previously observed in the birefringence data, the smallest anisotropy is exhibited by 6CB, while $\Delta\zeta$ increases with the chain length in case of 5CB and 7CB. This behavior again can be attributed to the before mentioned odd and even effect.

Figure 12.19b presents the polarizabilities for the ordinary and the extraordinary axis together with their mean value as a function of C atoms in the alkyl chain. As expected, the polarizabilities rise with the number of atoms in the alkyl chain. While in case of the mean values a linear increase by approximately 5% per CH_2 group is observed, the polarizabilities of the ordinary and the extraordinary axis reveal a strong impact of the odd and even effect: In case of 6CB, the additional CH_2 group mainly contributes to the short molecular axis, whereas the next odd member, i.e., 7CB, mainly strengthens the long axis.

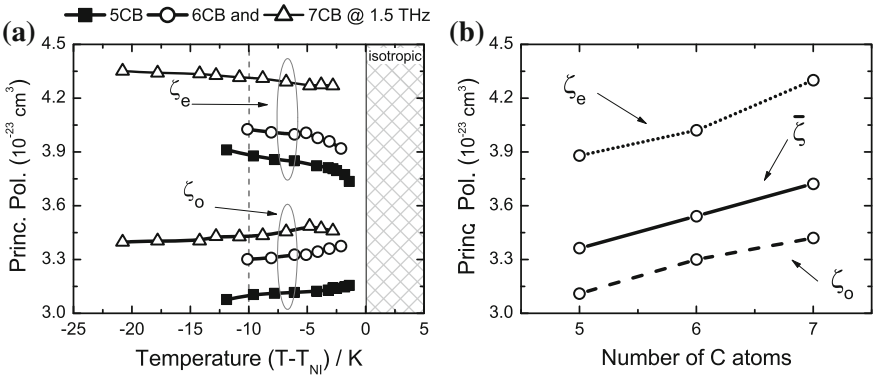

Fig. 12.19 **a** Principle polarizability of 5CB, 6CB, and 7CB at 1.5 THz calculated according to the Vuks's approximation and **b** Principle polarizability of 5CB, 6CB, and 7CB versus the number of C atoms in the alkyl chain. Data are taken from Fig. 12.19a at a reduced temperature of $T\text{-}T_{NI} = 10\,K$

12.1.10.4 Order Parameter S

The order parameter S is a relevant quantity to characterize the quality of parallel alignment of the LCs in the nematic phase. The S parameter equals unity at absolute zero, where all molecules show a perfect orientation. At temperatures above the phase transition T_{NI}, the S parameter equals zero. Here, the molecules exhibit a random orientation [102–107]. As long as thermal energy is left in the molecular system, i.e., at temperatures above absolute zero, the LC molecules have the ability to move around their center of mass. Hence, even in the nematic phase, despite the presence of an external electric field, only an average preferential orientation results instead of a perfect parallel alignment of all molecules.

To calculate the order parameter from the measured data we employ Haller's extension to Vuks' approximation, which can be written as follows [96, 98]:

$$S = \frac{n_e^2 - n_o^2}{\bar{n}^2 - 1} \frac{\bar{\zeta}}{\Delta\gamma} \tag{12.7}$$

Here, $\bar{\zeta}$ is the mean polarizability and $\Delta\gamma$ is the difference between the longitudinal and transverse polarizability components of the perfectly ordered molecule. In Fig. 12.20a we present the Haller plots ($S \cdot \Delta\gamma/\bar{\zeta}$) over the normalized reduced temperature $T_R = (T - T_{NI})/T_{NI}$ for 5CB, 6CB, and 7CB, respectively. In the low temperature regime, a linear dependence on a logarithmic scale is observed [98]. The order parameter S equals unity at $T = 0\,K$ (equivalent to $T_R = -1$) so that a graphical solution for the relative polarizability $\Delta\gamma/\bar{\zeta}$ can be obtained at the intercept of the extrapolated linear fit with the y-axis. For 5CB, 6CB, and 7CB the values of $\Delta\gamma/\bar{\zeta}$ are found to be 0.378, 0.401, and 0.375, respectively.

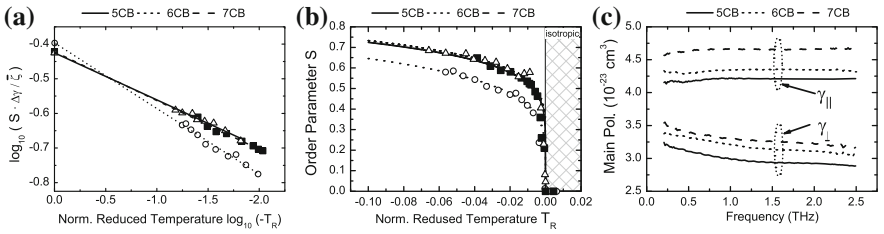

Fig. 12.20 **a** Haller plot of $S \cdot \Delta\gamma / \bar{\zeta}$ on the normalized reduced temperature T_R. **b** Order parameter S of 5CB, 6CB, and 7CB over the normalized reduced temperature τ obtained using Haller's extension to Vuks' approximation and **c** Frequency-dependent main polarizabilities of 5CB, 6CB, and 7CB

With the relative polarizabilities known, the order parameter S can be calculated according to equation (12.7). Figure 12.20b illustrates the dependence of the order parameter S on the normalized reduced temperature T_R for 5CB, 6CB, and 7CB. While the order parameter behaves similar for 5CB and 7CB, it is notably smaller in case of 6CB. This result agrees well with the results obtained by other authors and can be explained by the odd and even effect [108–111]. Molecules containing an odd number of C atoms in the alkyl chain show a higher flexibility than molecules with an even number of CH_2 groups. This behavior leads to a less uniform preferential orientation of the LCs [92].

12.1.10.5 Main Polarizabilities

Now that $\zeta_{e/o}$ and S are known, we will investigate the main polarizabilities of the molecules for the short and the long axis by applying equations (12.2) and (12.3). Figure 12.20c presents the main polarizabilities of 5CB, 6CB, and 7CB in the frequency range from 0.2 to 2.5 THz.

An additional alkyl chain member leads to more polarizability in both, the long and the short molecular axis. In accordance with the results from the study of the molecular structure, we found that odd members create a larger contribution to the polarizability of the molecular long axis, whereas even members contribute mainly to the molecular short axis due to the odd and even effect.

12.1.11 Summary and Outlook

To conclude, this work summarizes recent research performed on liquid crystals at THz frequencies. We presented macroscopic data in form of the refractive indices and the absorption coefficients of a variety of liquid crystals. The investigated substances comprise positive and negative dielectric anisotropy liquid crystals both in their pure form and in mixtures. Furthermore, we derived molecular properties such as the order

parameters S and the main polarizabilities from the macroscopic data using Haller's extension to Vuks' approximation.

One of the future challenges in this field lies in the implementation of liquid crystal-based THz devices, which overcome present drawbacks such as strong losses or slow switching times and which still give sufficient performance despite the low birefringence so far available at these frequencies.

Besides the investigation of new base materials, a paradigm change in the device design seems to become necessary: To avoid losses, instead of transmission-based structures the research should focus on devices operating in reflection mode. Furthermore, designs using only thin liquid crystal layers should be pursued, potentially involving artificial dielectrics such as photonic crystals or metamaterials to cope with the problem of the small interaction length. If innovative approaches are found, liquid crystal devices hold the potential to revolutionize THz technology in a similar, fundamental way as they already did in the optical regime.

References

1. F. Reinitzer, Beiträge zur kenntniss des cholesterins. Monatsh. Chem. **9**, 421–441 (1888)
2. M. Evans, M. Davies, I. Larkin, Molecular motion and molecular interaction in the nematic and isotropic phases of a liquid crystal compound. J. Chem. Soc., Faraday Trans. 2, **69**, 1011–1022 (1973)
3. B.J. Bulkin, W.B. Lok, Vibrational spectra of liquid crystals. V. far-infrared study of intermolecular modes in 4,4′-azoxydianisole and 4-methoxybenzylidene-4′-n-butylaniline. J. Phys. Chem. **77**, 326–330 (1973)
4. E. Sciesinska, J. Sciesinski, J. Twardowski, J.A. Janik, Absorption spectra of p-methoxy benzylidene p-n-butylaniline in the 80–400 cm^{-1} range at temperatures between −200 and 70 °C. Mol. Cryst. Liq. Cryst. **27**, 125–140 (1974)
5. M. Evans, R. Moutran, A.H. Price, Dielectric properties, refractive index and far infrared spectrum of cholesteryl oleyl carbonate. J. Chem. Soc., Faraday Trans. 2, **71**, 1854–1862 (1975)
6. S. Venugopalan, J.R. Fernandes, G.V. Vani, Far-infrared and raman spectra of the solid phases of CBOOA. Mol. Cryst. Liq. Cryst. **31**, 29–46 (1975)
7. G.J. Evans and M. Evans, High and low frequency torsional absorptions in nematic K21. J. Chem. Soc., Faraday Trans. 2, **73**, 285–292 (1976)
8. J.R. Fernandes, S. Venugopalan, Infrared spectroscopic study of orientational order and phase transformations in liquid crystalline CBOOA. Mol. Cryst. Liq. Cryst. **35**, 113–134 (1976)
9. S. Venugopalan, J.R. Fernandes, V. Surendranath, Far-infrared absorption in the highly ordered smectic phases of TBBA. Mol. Cryst. Liq. Cryst. **40**, 149–161 (1977)
10. G.J. Evans, M.W. Evans, Far-infrared spectroscopy of liquid crystals. Infrared Phys. **18**, 863–866 (1978)
11. A. Buka, G.P. Owen, A.H. Price, Dielectric relaxation in the nematic and isotropic phases of n-heptyl- and n-heptoxy-cyanobiphenyl. Mol. Cryst. Liq. Cryst. **51**, 273–284 (1979)
12. C.J. Reid, M.W. Evans, Assignment of far infrared absorptions in liquid crystalline 4-n-heptyl-4'-cyanobiphenyl. Mol. Phys. **40**, 1523–1526 (1980)
13. D. Decoster, J. Depret, Determination du parametre d'ordre de quelques composes nematiques a l'aide d'un laser submillimetrique. Mol. Cryst. Liq. Cryst. **56**, 151–156 (Jan. 1980)
14. G.J. Evans, Collective modes in a nematic liquid crystal. J. Chem. Soc., Faraday Trans. 2, **79**, 833–845 (1983)

15. J. Shashidhara Prasad, M.M.M. Abdoh, C.I. Venkataramana Shastry, N.C. Shivaprakash, Infrared and far-infrared studies on the nematogenic homologous series trans-4-alkyl-(4-cyanobiphenyl)cyclohexanes. Mol. Cryst. Liq. Cryst. **104**, 141–152 (1984)
16. G.J. Evans, K. Moscicki, The poley absorption in liquid crystals. J. Mol. Liq. **32**, 149–160 (1986)
17. U.M.S. Murthy, J.K. Vij, Submillimetre wave spectroscopy of 4-n-alkyl-4'-cyano biphenyl liquid crystals. Liq. Cryst. **4**, 529–542 (1989)
18. T. Nose, S. Sato, K. Mizuno, J. Bae, T. Nozokido, Refractive index of nematic liquid crystals in the submillimeter wave region. Appl. Opt. **36**, 6383–6387 (1997)
19. D. Turchinovich, P. Knobloch, G. Luessem, M. Koch, THz time-domain spectroscopy on 4-(trans-4'-pentylcyclohexyl)-benzonitril, *Proceedings of SPIE*, ed. by I.C. Khoo, vol. 4463, 2001, pp. 65–70
20. R.P. Pan, T.R. Tsai, C.Y. Chen, C.L. Pan, Optical constants of two typical liquid crystals 5CB and PCH5 in the THz frequency range. J. Biol. Phys. **29**, 335–338 (2003)
21. R.P. Pan, T.R. Tsai, C.Y. Chen, C.H. Wang, C.L. Pan, The refractive indices of nematic liquid crystal 4'-n-Pentyl-4-cyanobiphenyl in the THz frequency range. Mol. Cryst. Liq. Cryst. **409**, 137–144 (2004)
22. C.L. Pan, R.P. Pan, Recent progress in liquid crystal THz optics, *Proceedings of SPIE*, ed. by L.C. Chien, vol. 6135, 2006, p. 61350D
23. R.P. Pan, C.F. Hsieh, C.L. Pan, C.Y. Chen, Temperature-dependent optical constants and birefringence of nematic liquid crystal 5CB in the terahertz frequency range. J. Appl. Phys. **103**, 093523 (2008)
24. V.V. Meriakri, C.L. Pan, R.P. Pan, M.P. Parkhomenko, E.E. Chigrai, in Measurement of dielectric properties of liquid crystals in the THz range, *Proccedings of the Conference on Advanced Optoelectronics and Lasers*, Alushta, Ukraine 2008, pp. 109–111
25. V.V. Meriakri, E.E. Chigray, C.L. Pan, R.P. Pan, M.P. Parkhomenko, in Dielectric properties of liquid crystals in the terahertz frequency range, *Proceedings of the International Conference on Infrared, Millimeter, and Terahertz Waves*, IRMMW/THz, Busan, South Korea, 2009
26. C.Y. Chen, C.F. Hsieh, Y.F. Lin, R.P. Pan, C.L. Pan, Magnetically tunable room-temperature 2 pi liquid crystalterahertz phase shifter. Opt. Express **12**, 2630–2635 (2004)
27. C.S. Yang, C.J. Lin, R.P. Pan, C.T. Que, K. Yamamoto, M. Tani, C.L. Pan, The complex refractive indices of the liquid crystal mixture E7 in the terahertz frequency range. J. Opt. Soc. Am. B **27**, 1866–1873 (2010)
28. T.T. Tan, R.P. Pan, Y.C. Wang, C.L. Pan, THz time-domain spectroscopic studies of a ferroelectric liquid crystal in the SmA* and SmC* Phases. Ferroelectrics **1**, 72–77 (2008)
29. M. Oh-e, H. Yokoyama, M. Koeberg, E. Hendry, M. Bonn, High-frequency dielectric relaxation of liquid crystals: THz time-domain spectroscopy of liquid crystal colloids. Opt. Express **14**, 11433–11440 (2006)
30. Y. Takanishi, K. Ishikawa, J. Watanabe, H. Takezoe, M. Yamashita, K. Kawase, Terahertz spectroscopy in smectic phases of a bent-core molecule. Phys. Rev. E **71**, 2–4 (2005)
31. J.I. Nishizawa, T. Yamada, T. Sasaki, T. Tanabe, T. Wadayama, T. Tanno, K. Suto, Terahertz dichroism of MBBA liquid crystal on rubbed substrate. Appl. Surf. Sci. **252**, 4226–4229 (2006)
32. F. Rutz, T. Hasek, M. Koch, H. Richter, U. Ewert, Terahertz birefringence of liquid crystal polymers. Appl. Phys. Lett. **89**, 221911 (2006)
33. R. Wilk, N. Vieweg, O. Kopschinski, T. Hasek, M. Koch, THz spectroscopy of liquid crystals from the CB family. J. Infrared Milli Terahz Waves **30**, 1139–1147 (2009)
34. N. Vieweg, M.K. Shakfa, B. Scherger, M. Mikulics, M. Koch, THz properties of nematic liquid crystals. J. Infrared Milli Terahz Waves **31**, 1312–1320 (2010)
35. N. Vieweg, M.K. Shakfa, M. Koch, BL037: a nematic mixture with high terahertz birefringence. Opt. Commun. (2011)
36. N. Vieweg, M. Koch, Terahertz properties of liquid crystals with negative dielectric anisotropy. Appl. Opt. **49**, 5764–5767 (Oct. 2010)

37. O. Trushkevych, H. Xu, T. Lu, J.A. Zeitler, R. Rungsawang, F. Gölden, N. Collings, W.A. Crossland, Broad spectrum measurement of the birefringence of an isothiocyanate based liquid crystal. Appl. Opt. **49**, 5212–5216 (2010)
38. C.Y. Chen, T.R. Tsai, C.L. Pan, R.P. Pan, Room temperature terahertz phase shifter based on magnetically controlled birefringence in liquid crystals. Appl. Phys. Lett. **83**, 4497–4499 (2003)
39. T.R. Tsai, C.Y. Chen, R.P. Pan, C.L. Pan, X.C. Zhang, Electrically controlled room temperature terahertz phase shifter with liquid crystal. IEEE Microwave Wirel. Compon. Lett. **14**, 77–79 (2004)
40. H.Y. Wu, C.F. Hsieh, T.T. Tang, R.P. Pan, C.L. Pan, Electrically tunable room-temperature 2 pi liquid crystal terahertz phase shifter. IEEE Photonics Technol. Lett. **18**, 1488–1490 (Jul. 2006)
41. C.L. Pan, C.F. Hsieh, R.P. Pan, M. Tanaka, F. Miyamaru, M. Tani, M. Hangyo, Control of enhanced THz transmission through metallic hole arrays using nematic liquid crystal. Opt. Express **13**, 3921–3930 (2005)
42. C.Y. Chen, C.L. Pan, C.F. Hsieh, Y.F. Lin, R.P. Pan, Liquid-crystal-based terahertz tunable lyot filter. Appl. Phys. Lett. **88**, 101107 (2006)
43. C.F. Hsieh, Y.C. Lai, R.P. Pan, C.L. Pan, Polarizing terahertz waves with nematic liquid crystals. Opt. Lett. **33**, 1174–1176 (2008)
44. C.J. Lin, Y.T. Li, C.F. Hsieh, R.P. Pan, C.L. Pan, Manipulating terahertz wave by a magnetically tunable liquid crystal phase grating. Opt. Express **16**, 2995–3001 (2008)
45. H. Zhang, P. Guo, P. Chen, S. Chang, J. Yuan, Liquid-crystal-filled photonic crystal for terahertz switch and filter. J. Opt. Soc. Am. B **26**, 101–106 (2009)
46. R. Wilk, N. Vieweg, O. Kopschinski, M. Koch, Liquid crystal based electrically switchable bragg structure for THz waves. Opt. Express **17**, 7377–7382 (2009)
47. Z. Ghattan, T. Hasek, R. Wilk, M. Shahabadi, M. Koch, Sub-terahertz on-off switch based on a two-dimensional photonic crystal infiltrated by liquid crystals. Opt. Comm. **281**, 4623–4625 (2008)
48. I.C. Khoo, D.H. Werner, X. Liang, A. Diaz, Nanosphere dispersed liquid crystals for tunable negative—Zero—positive index of refraction in the optical and terahertz regimes. Opt. Lett. **31**, 2592–2594 (2006)
49. X. Wang, D-H. Kwon, D.H. Werner, I-C. Khoo, A.V. Kildishev, V.M. Shalaev, Tunable optical negative-index metamaterials employing anisotropic liquid crystals. Appl. Phys. Lett. **91**, 143122 (2007)
50. S. Xiao, U.K. Chettiar, A.V. Kildishev, V. Drachev, I.C. Khoo, V.M. Shalaev, Tunable magnetic response of metamaterials. Appl. Phys. Lett. **95**, 033115 (2009)
51. D.H. Werner, D.H. Kwon, I.C. Khoo, A.V. Kildishev, V.M. Shalaev, Liquid crystal clad near-infrared metamaterials with tunable negativ-zero-positive refractive indices. Opt. Express **15**, 3342–3347 (2007)
52. Q. Zhao, L. Kang, B. Du, B. Li, J. Zhou, H. Tang, X. Liang, B. Zhang, Electrically tunable negative permeability metamaterials based on nematic liquid crystals. Appl. Phys. Lett. **90**, 011112 (2007)
53. J.A. Bossard, X. Liang, L. Li, S. Yun, D.H. Werner, B. Weiner, T.S. Mayer, P.F. Cristman, A. Diaz, I.C. Khoo, Tunable frequency selective surfaces and negative-zero-positive index metamaterials based on liquid crystals. IEEE Trans. Antennas Propag. **56**, 1308–1320 (2008)
54. Y. Yuan, J. He, J. Liu, J. Yao, Proposal of an electrical controlled terahertz switch based on liquid-crystal-filled dual-metallic grating structures. Appl. Opt. **49**, 6092–6097 (2010)
55. S. Singh, Phase transitions in liquid crystals. Phys. Rep. **324**, 107–269 (2000)
56. D. Pauluth, K. Tarumi, Advanced liquid crystals for television. J. Mater. Chem. **14**, 1219–1227 (2004)
57. P. Kirsch, V. Reiffenrath, M. Bremer, Nematic liquid crystals with negative dielectric anisotropy: molecular design and synthesis. Synlett **1999**, 389–396 (1999)
58. V. Reiffenrath, J. Krause, H.J. Plach, G. Weber, New liquid-crystalline compounds with negative dielectric anisotropy. Liq. Cryst. **5**, 159–170 (1989)

59. P. Kula, A. Spadlo, J. Dziaduszek, M. Filipowicz, R. Dabrowski, J. Czub, S. Urban, Mesomorphic, dielectric, and optical properties of fluorosubstituted biphenyls, terphenyls, and quaterphenyls. Opto-Electron. Rev. **16**, 379–385 (2008)
60. S. Gauza, S.T. Wu, A. Spadło, R. Dabrowski, High performance room temperature nematic liquid crystals based on laterally fluorinated isothiocyanato-tolanes. J. Disp. Technol. **2**, 247–253 (2006)
61. Q. Song, S. Gauza, H. Xianyu, S.T. Wu, Y.M. Liao, C.Y. Chang, C.S. Hsu, High birefringence lateral difluoro phenyl tolane liquid crystals. Liq. Cryst. **37**, 139–147 (2010)
62. R.D. Dabrowski, J. Dziaduszek, A. Ziolek, Ł. Szczucinski, Z. Stolarz, G. Sasnouski, V. Bezborodov, W. Lapanik, S. Gauza, S.T. Wu, Low viscosity, high birefringence liquid crystalline compounds and mixtures. Opto-Electron. Rev. **15**, 47–51 (2007)
63. S. Gauza, C.H. Wen, B. Tan, S.T. Wu, UV stable high birefringence liquid crystals. Jpn. J. Appl. Phys. **43**, 7176–7180 (2004)
64. T.N. Soorya, S. Gupta, A. Kumar, S. Jain, V.P. Arora, B. Bahadur, Temperature dependent optical property studies of nematic mixtures. Indian J. Pure Appl. Phys. **44**, 524–531 (2006)
65. B. Gestblom, S. Wrobel, A thin cell dielectric spectroscopy method for liquid crystals. Liq. Cryst. **18**, 31–35 (1995)
66. C. Weil, S. Mu, P. Scheele, P. Best, G. Luessem, R. Jakoby, Highly-anisotropic liquid-crystal mixtures for tunable microwave devices. Electron. Lett. **39**, 26–28 (2003)
67. S.T. Wu, Absorption measurements of liquid crystals in the ultraviolet, visible, and infrared. J. Appl. Phys. **84**, 4462–4465 (1998)
68. J. Li, S.T. Wu, Extended cauchy equations for the refractive indices of liquid crystals. J. Appl. Phys. **95**, 896–901 (2004)
69. D. Grischkowsky, S. Keiding, M. Van Exter, C. Fattinger, Far-infrared time-domain spectroscopy with terahertz beams of dielectrics and semiconductors. J. Opt. Soc. Am. B **7**, 2006–2015 (1990)
70. P.U. Jepsen, R.H. Jacobsen, S.R. Keiding, Generation and detection of terahertz pulses from biased semiconductor antennas. J. Opt. Soc. Am. B **13**, 2424–2436 (1996)
71. P.U. Jepsen, D.G. Cooke, M. Koch, Terahertz spectroscopy and imaging—modern techniques and applications. Laser Photonics Rev. 1–43, (2010)
72. N. Vieweg, M. Mikulics, M. Scheller, K. Ezdi, R. Wilk, H. Hübers, M. Koch, Impact of the contact metallization on the performance of photoconductive THz antennas. Opt. Express **16**, 19695–19705 (2008)
73. N. Vieweg, C. Jansen, M.K. Shakfa, M. Scheller, N. Krumbholz, R. Wilk, M. Mikulics, M. Koch, Molecular properties of liquid crystals in the terahertz frequency range. Opt. Express **18**, 6097–107 (2010)
74. R. Wilk, I. Pupeza, R. Cernat, M. Koch, Highly accurate THz time-domain spectroscopy of multy-layer structures. IEEE J. Sel. Top. Quantum Electron. **14**, 392–398 (2008)
75. M. Scheller, C. Jansen, M. Koch, Analyzing sub-100- μm samples with transmissionterahertz time domain spectroscopy. Opt. Comm. **282**, 1304–1306 (2009)
76. C. Jansen, S. Wietzke, H. Wang, M. Koch, G. Zhao, Terahertz spectroscopy on adhesive bonds. Polym. Testing **30**, 150–154 (2011)
77. G.W. Gray, K.J. Harrison, J.A. Nash, New family of nematic liquid crystals for displays. Electron. Lett. **9**, 130–131 (1973)
78. R.V. Eidenschink, D. Erdmann, J. Krause, L. Pohl, Substituierte phenylcyclohexane-eine neue klasse flüssigkristalliner verbindungen. Angew. Chem. **89**, 103 (1977)
79. L. Pohl, R. Eidenschink, G. Krause, D. Erdmann, Physical properties of nematic phenylcyclohexanes, a new class of low melting liquid crystals with positive dielectric anisotropy. Phys. Lett. **60A**, 421–423 (1977)
80. U. Finkenzeller, T. Geelhaar, G. Weber, L. Pohl, Liquid-crystalline reference compounds. Liq. Cryst. **5**, 313–321 (1989)
81. D.A. Dunmur, D.A. Hitchen, X.J. Hong, The Physical and Molecular Properties of some Nematic Fluorobiphenylalkanes. Mol. Cryst. Liq. Cryst. **140**, 303–318 (Nov. 1986)

82. R. Dabrowski, J. Jadzyn, J. Dziaduszek, Z. Stolarz, G. Czechowski, M. Kasprzyka, The physical and molecular properties of new low melting nematics with negative dielectric anisotropy. Z. Naturforsch. **52**, 448–450 (1999)
83. R. Dabrowski, J. Jadzyn, S. Czerkas, J. Dziaduszek, A. Walczak, New low melting nematics 2-chloro-4-alkylphenyl 4-alkylbicyclo-[2,2,2]octane-1-carboxylates with negative dielectric anisotropy. Mol. Cryst. Liq. Cryst. **332**, 61–68 (Aug. 1999)
84. Technical Datasheet of MLC7029, Merck KGaA
85. J. Dziaduszek, R. Dabrowski, A. Zióek, S. Gauza, and S.T. Wu, Syntheses and mesomorphic properties of laterally fluorinatedphenyl isothiocyanatotolanes and their high birefringent mixtures. Opto-Electron. Rev. **17**, 20–24 (2009)
86. V. Vill, *Liquid Crystal Database 4.6* (LCI Publischer, Hamburg, 2005)
87. M.I. Capar, E. Cebe, Odd—even effects in the homologous series of alkyl-cyanobiphenyl liquid crystals: a molecular dynamic study. J. Comput. Chem. **28**, 2140–2146 (2007)
88. M.I. Capar, E. Cebe, Molecular dynamic study of the odd-even effect in some 4-n-alkyl-4'-cyanobiphenyls. Phys. Rev. E. **73**, 061711 (2006)
89. P. Forstert, B.M. Fung, Chain ordering in cyanobiphenyls and cyanophenylcyclohexanes. J. Chem. Soc., Faraday Trans. 2. **84**, 1083–1094 (1988)
90. S. Marcelja, Chain ordering in liquid crystals. I. even-odd effect. J. Chem. Phys. **60**, 3599–3604 (1974)
91. J.R. Lalanne, J.C. Rayez, B. Duguay, A. Proutiere, R. Viani, Molecular aspects of the even-odd effect in cyanobiphenyls (nCB): theoretical studies of the molecular geometrical conformation and optical anisotropy. J. Chem. Phys. **81**, 344–348 (1984)
92. I. Chirtoc, M. Chirtoc, C. Glorieux, J. Thoen, Determination of the order parameter and its critical exponent for nCB ($n = 5 - 8$) liquid crystals from refractive index data. Liq. Cryst. **31**, 229–240 (2004)
93. I. Cacelli, L.D. Gaetani, G. Prampolini, A. Tani, Liquid crystal properties of the n-alkyl-cyanobiphenyl series from atomistic simulations with ab initio derived force fields. J. Phys. Chem. B **111**, 2130–2137 (2007)
94. M.I. Capar, E. Cebe, Rotational viscosity in liquid crystals: a molecular dynamics study. Chem. Phys. Lett. **407**, 454–459 (2005)
95. N.C. Shashidhara Prasad, M.M.M. Abdoh, Srinivasa, J. Shashidhara Prasad, Refractive indices, densities, polarizabilities and molecular order in cholesteric liquid crystals. Mol. Cryst. Liq. Cryst. **80**, 179–193 (1982)
96. R.G. Horn, Refractive indices and order parameters of two liquid crystals. J. Phys. **39**, 105–109 (1978)
97. M.F. Vuks, Determination of the optical anisotropy of aromatic molecules from the double refraction of crystals. Opt. Spektrosk. **20**, 644–651 (1966)
98. I. Haller, Thermodynamic and static properties of liquid crystals. Solid-State Chem. **10**, 103–118 (1975)
99. C.J.F. Böttcher, *Theory of Electric Polarisation* (Elsevier, Amsterdam, 1952)
100. S. Chandrasekhar, N.V. Madhusudana, Orientational order in p-azoxyanisole, p-azoxyphenetole and their mixtures in the nematic phase. J. Phys. Colleq. **30**, C4–24 (1969)
101. Group Landolt-Börnstein, *Group VIII Advanced Materials and Technologies Physical Properties of Liquid Crystals* (Springer, Berlin, 2003)
102. W. Maier, A. Saupe, Eine einfache molekulare theorie des nematischen kristallinen zustandes. Z. Naturforsch. A. **13** 564 (1958)
103. W. Maier, A. Saupe, Eine einfache molekularstatistische theorie der nematischen kristallinflüssigen phase teil I. Z. Naturforsch. A. **14**a, 882 (1959)
104. M.J. Freiser, Ordered states of a nematic Liquid. Phys. Rev. Lett. **24**, 1041–1043 (1970)
105. J.R. McColl, C.S. Shih, Temperature dependence of orientational order in a nematic liquid crystal at constant molar volume. Phys. Rev. Lett. **29**, 85–87 (1972)
106. G. Heppke, C. Bahr, *Aufbau der Materie* (W. de Gruyter, Berlin, 1981)
107. P.J. Collings, M. Hird, *Introduction to Liquid Crystals Chemistry and Physics* (Taylor & Francis, London, 2004)

108. S. Urban, A. Würflinger, B. Gestblom, On the derivation of the nematic order parameter from the dielectric relaxation times. Phys. Chem. Chem. Phys. **1**, 2787–2791 (1999)
109. A. Buka, W.H. De Jeu, Diamagnetism and orientational order of nematic liquid crystals. J. Phys. Chem. **43**, 361–367 (1982)
110. J.A. Ratto, S. Ristori, F. Volino, M. Pineri, M. Thomas, M. Escoubes, R.B. Blumstein, Investigation of a liquid crystal dispersed in an ionic polymeric membrane. Chem. Mater. **5**, 1570–1576 (1993)
111. I.H. Ibrahim, W. Haase, On the molecular polarizability of nematic liquid crystals. Mol. Cryst. Liq. Cryst. **66**, 189–198 (1981)